ABSTRACT

Errors in Constant-Velocity Shaft Couplings

by
Philip M. Remington

A Multiloop spatial system of rotations is used to represent a shaft coupling, allowing a transmission plane which may deviate from the plane of symmetry to be specified. The plane of transmissión, for intersecting input and output shaft axes, is the locus of intersections of screw axes that compose the system. By prescribing the transmission plane outside of the plane of symmetry (commonly called the "homokinetic plane" or "bisecting plane") to specified orientations, a phase shift between the input and output shaft rotational displacements will be quantified. The rotational phase shift between the input and output shafts can be evaluated for a series of configurations to classify the critical deviations from constant-velocity transmission as a function of the transmission plane location.

ERRORS IN CONSTANT-VELOCITY SHAFT COUPLINGS

by
Philip M. Remington

A Thesis
Submitted to the Faculty of
New Jersey Institute of Technology
in Partial Fulfillment of the Requirements for the Degree of
Masters of Science in Mechanical Engineering
October, 1992

APPROVAL PAGE

Errors in Constant-Velocity Shaft Couplings

by
Philip M. Remington

9/1/92

Dr. Ian S. Fischer, Thesis Adviser
Associate Professor of Mechanical Engineering, NJIT

9/1/92

Dr. Rajesh N. Dave, Committee Member
Associate Professor of Mechanical Engineering, NJIT

Sept 1, 1992

Dr. Anthony D. Rosato, Committee Member
Assistant Professor of Mechanical Engineering, NJIT

BIOGRAPHICAL SKETCH

Author: Philip M. Remington

Degree: Master of Science in Mechanical Engineering

Date: October 1992

Date of Birth:

Place of Birth:

Undergraduate and Graduate Education:

- Master of Science in Mechanical Engineering,
  New Jersey Institute of Technology, Newark, N.J. 1992

- Bachelor of Science in Mechanical Engineering,
  New Jersey Institute of Technology, Newark, N.J. 1990

Major: Mechanical Engineering

TABLE OF CONTENTS

LIST OF FIGURES

CHAPTER 1
INTRODUCTION

1.1 Overview

A constant-velocity shaft coupling, often refered to as a CV shaft coupling, ideally provides constant-velocity transmission between two non-colinear shafts. Because of wear and manufacturing tolerances, CV shaft couplings may deviate from the ideal geometry which produces constant output speed for a constant input speed. This study is concerned with calculating the fluctuation in the output-shaft speed, relative to the input-shaft speed, when the dimensional differences between the ideal and actual geometry of the CV shaft coupling are known. A CV shaft coupling mathematical model is developed which allows the dimensional differences between the ideal and actual geometry to be specified. This model is then evaluated for fluctuations in the output-shaft speed relative to the input-shaft speed subject to various actual geometric possibilities. This mathematical model will allow the design engineer to directly correlate the CV shaft coupling dimensional tolerances and the deviation from constant velocity performance. It will also lead to a better understanding of the wear patterns in the coupling components.

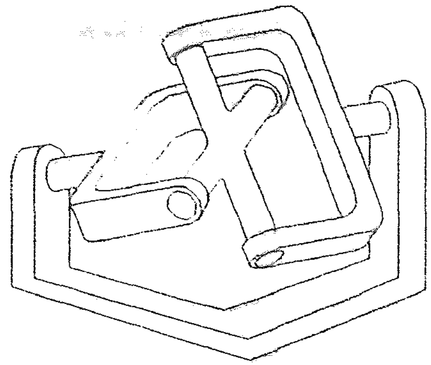

Fig. 1 - 1 The Cardan or Hooke joint is the most common shaft coupling for rotational transmission through two shafts whose axes of rotation intersect.

1.2 Definition of Shaft Coupling

Shaft Couplings are mechanisms used to transmit rotational displacement between two shafts whose axes of rotation are not collinear. The angle between the two shaft axes of rotation is refered to as the shaft angle. The most common shaft coupling in use is the Cardan or Hooke joint, shown in Fig. 1-1, which consists of four perpendicular revolute joints in series whose axes of rotation intersect at a point. The Cardan joint be more easily observed if redundant revolute joints are omitted, as represented in Fig. 1-2. The Cardan joint is not a constant-velocity coupling, as there will be a cyclic variation in the output-shaft speed relative to a constant input-shaft speed. The cyclic variation can be derived as a function of the frame angle, for a given shaft coupling.

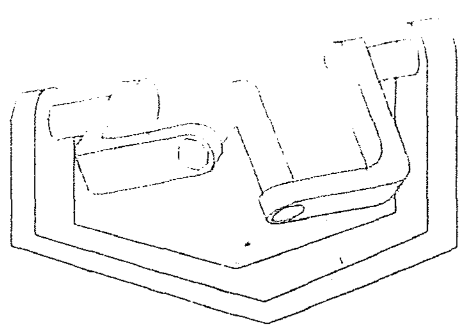

Fig. 1 - 2 The Cardan or Hooke joint can be reduced to this form, remaining faithful to the kinematic design. This representation shows the essential kinematic structure, consisting of four perpendicular revolute joints in series. All four revolute joint axes must intersect at a single point.

1.3 Definition of Constant-Velocity Coupling

A constant-velocity shaft coupling is designed such that the output shaft always rotates at the same speed as the input shaft. The general characteristics of constant-velocity shaft couplings has been a topic of great interest to theoretical kinematics researchers and automotive engineers alike (*Freudenstein and Maki* 1979, *Steeds* 1937). A brief discussion of existing CV shaft couplings will assist in understanding the design requirements. Constant-velocity shaft couplings, often called "constant-velocity universal joints", have been extensively used in front wheel automobile drives and this application has led to many advancements in CV shaft coupling design.

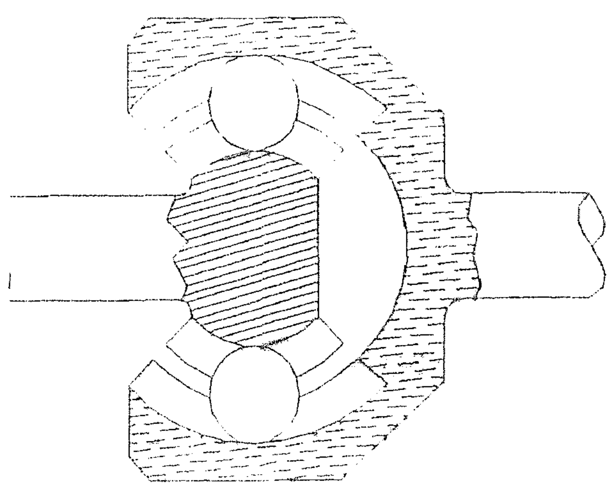

Fig. 1 - 3 This sliced view of a simplified Rzeppa CV shaft coupling shows the application of ball-groove joints. Four other balls are situated similarly about the shaft coupling. The center of curvature of all spherical grooves meet at the intersection of shaft axes.

The most popular constant-velocity couplings for shafts whose axes of rotation intersect at a point are those with ball-groove joints which have compactness, precision and durability (*Miller* 1965). The ball-groove joint was first recognized as a viable option for constant velocity shaft couplings in the late 1920's. Although a large variety of CV shaft coupling designs came from *F. E. Myard* (1933), *A. H. Rzeppa* (1928) was recognized as the innovator of the ball-groove CV shaft coupling. A Rzeppa constant-velocity shaft coupling contains six balls in spherical grooves. These grooves are made concentric about the intersection of the two shaft axes of rotation. The balls are forced against the grooves, which transmits torque between the input shaft and the output shaft (*H. H. Mabie* 1948).

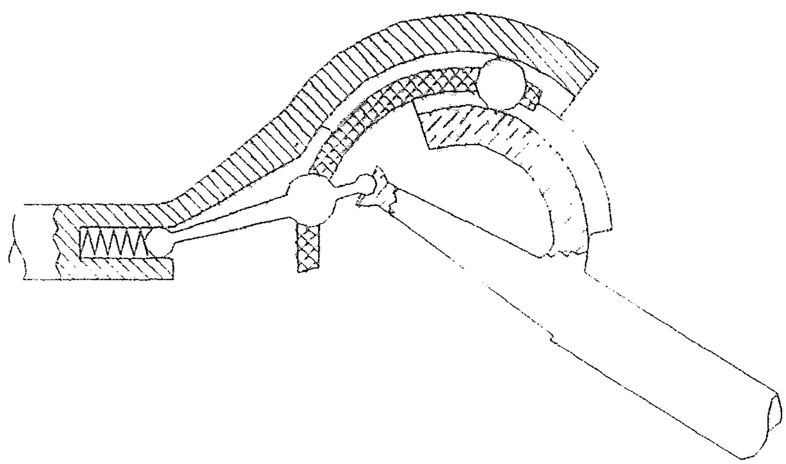

Fig. 1 - 4 This sliced piece of a Rzeppa CV shaft coupling shows the ball cage, directed by the spring loaded pilot lever, positioning a ball in a position symmetric to both the input shaft and the output shaft.

The success of the Rzeppa CV shaft coupling is contingent on the precise positioning of the balls in a plane symmetric to both shafts. This plane is called the homokinetic or bisecting plane. This was first accomplished by using a ball cage directed by a spring loaded pilot lever (*Rzeppa* 1928). This ball positioning mechanism can approximately position the balls in the homokinetic plane, which leads to the investigation of the deviation from constant velocity due to errors in this approximation.

Later patents on the Rzeppa CV shaft coupling involving eccentric and non-spherical ball grooves lead to ball positioning without need for a pilot lever (*Rzeppa* 1934,1935). For these designs the tolerances in the grooves must be very precise, to maintain acceptable constant-velocity transmission. These designs adhere to the principle of the homokinetic plane so the mathematical model that follows remains valid. The deviation from constant-velocity transmission can be attributed to the deviation of the balls from the homokinetic plane.

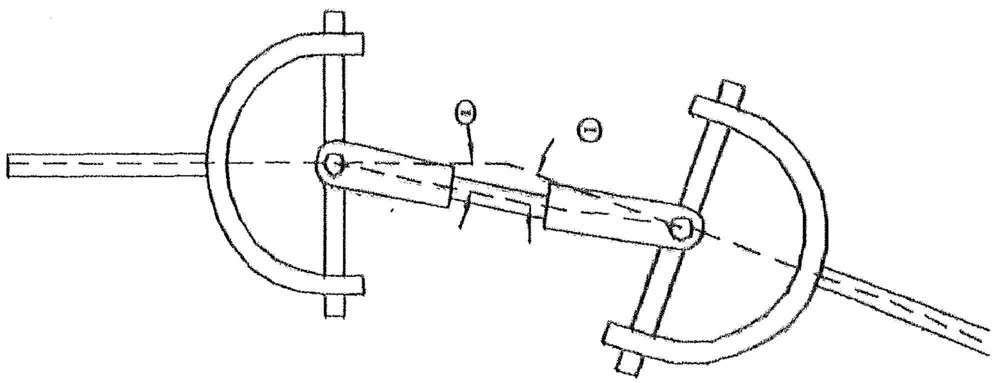

Fig. 1 - 5 The double Cardan joint configured with equally opposite shaft angles of can produce a sum rotational phase shift of zero between the input shaft and the output shaft.

There are two basic classes of constant-velocity shaft couplings. One class includes the double-Cardan joint driveline which has been extensively studied by *Fischer and Paul* (1987) and the double-pode joint driveline by *Akbil and Lee* (1983). These drivelines operate on the premise that two non-constant-velocity couplings configured in series at equally opposite angles will produce a sum rotational phase shift of zero.

The other class of CV shaft couplings, which is of primary interest to this study, produces constant-velocity through shafts, whose axes of rotation intersect at a point. This class of shaft couplings operate on the principle of the homokinetic plane. The homokinetic plane is the plane symmetric to both the input and output shafts, where the location of transmission between the shafts must occur for constant-velocity transmission (*Sturges* 1947). Most of all known mechanisms which comprise this class have been derived by *Freudenstein and Maki* (1979) using a graph-theory synthesis method.

This graph-theory synthesis method consists of reducing all mechanisms to fundamental components, where rigid bodies are represented by vertices(points) and joints which connect the rigid bodies are represented by edges(lines) which connect the corresponding vertices. The variety of constant-velocity couplings derived, includes the Tracta, Clemens, Altman, Myard and Rzeppa plus some of which have not been implemented into practice. This graph-theory synthesis method revelled several possible combinations of joints, all of which follow the principle of the homokinetic plane.

The principle of the homokinetic plane more specifically includes kinematic requirements in addition to the fundamental geometric requirements. As noted in *Hunt* (1973), the theory of shaft couplings designed to produce constant-velocity transmission, requires an odd number of joints arrayed equally about a central axis. A central joint in the coupling must be located in the plane of symmetry between the input and output shafts, commonly called the "homokinetic plane" or "bisecting Plane", to achieve constant-velocity transmission. This plane of symmetry must also contain the intersection of the axes of the joints configured about it. Two examples of CV shaft couplings which explicitly show these requirements, discussed later, are shown in Fig. 1-7. As the homokinetic plane is the ideal location of transmission, the actual plane of transmission will be refered to as the transmission plane. The transmission plane ideally coincides with the homokinetic plane, however in actuality this is not the case. The effect on constant-velocity transmission due to the deviation of the transmission plane from the homokinetic plane is developed here.

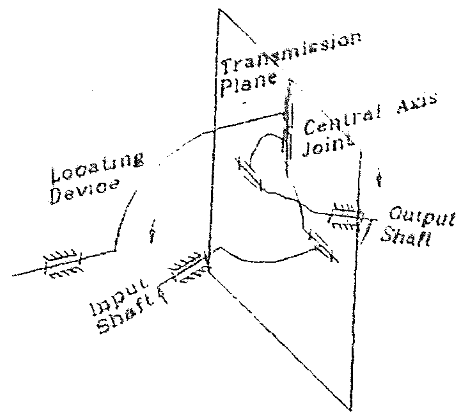

Fig. 1 - 6 Spherical construction of CV shaft coupling with external locating device positioning the central axis joint in the plane of transmission.

1.4 Description of Model

As noted in *Freudenstein and Maki* (1979), the sum of the freedoms of the joints in a spatially derived CV shaft coupling must be seven to maintain the needed symmetry and freedoms. This note is relevant only for spatial mechanisms. The mathematical model is developed in spherical space and need possess five rotational freedoms in the shaft coupling with specialized constraints for positioning the transmission plane. This configuration was alluded to by *Hunt* (1973) in an approach to synthesize a high-precision general CV coupling composed of lower pairs with the minimum number of freedoms. This configuration, like the well-known Rzeppa (*Rzeppa* 1953) or Bendix-Weiss (*Sturges* 1947) ball groove type CV shaft couplings, operates on the principle of the homokinetic plane.

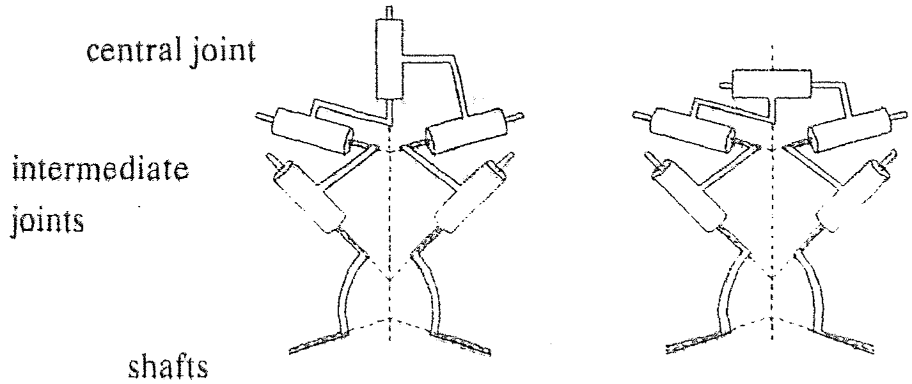

Fig. 1 - 7 (a) & (b) These mechanisms consist of seven revolute joints arrayed equally about a central axis symmetric to the input and output shafts, which satisfies the principle of the homokinetic plane.

The 7R(seven revolute joints in series) spatial mechanisms, shown in Fig. 1-7, suitable for constant-velocity transmission, originally introduced by *Myard* (1933), are thoroughly discussed by *Hunt* (1973). Spherical space, which simplifies the system, can be achieved by projecting the spatial system of orthogonal rotations in Fig. 1-7 (a), declaring all axes intersect at a point, on that point, where all distances degenerate from the mechanism. This transformation, accomplished by representing the two intermediate joints on each side of the mechanism as single linearly independent joints, satisfies the mobility criteria in spherical space. More simply, the transformation between any two axes in spherical space can be represented by a single rotation about an axis linearly independent to both axes. This holds true for the transformation between the axes of the central joint and each shaft. This kinematic rule helps describe the reduction of a one degree-of-freedom, 7R spatial mechanism to a two degree-of-freedom, 5R spherical mechanism with out violating the principle of the homokinetic plane, when the central joint is externally constrained to the homokinetic plane. The additional degree-of-freedom will be utilized to locate the transmission plane independent of the shaft locations. The prospect of utilizing this construction as a means of analyzing the errors in couplings that operate on the principle of the homokinetic plane does prove to be effective. The deviation from constant-velocity transmission of the CV shaft coupling when the orientation of the transmission plane leaves the bisecting plane or homokinetic plane is the focus of this study.

1.5 Motivation

For Rzeppa CV shaft couplings the motion of the pilot lever and clearance of the ball grooves, determine the position of the transmission plane. Contact between the balls and ball grooves in these couplings are the primary location of fatigue (*Sutherland* 1976, *Macielinski* 1970). Wear and manufacturing-tolerance deviations from ideal geometry induce output speed fluctuation in what was intended as a constant-velocity coupling. These limitations inspire a need to investigate in detail the effect of the manufacturing tolerances and wear on the ability of the CV shaft coupling to transmit constant-velocity.

By developing a technique, to relate geometric aspects like ball-groove clearances and the pilot lever motion accuracy to the input/output shaft rotational displacement, a better evaluation of designs will be possible. This model is developed on the premise that the transmission plane can be located independent of the shaft locations. This will allow the model to evaluate the effect of specific locations of the transmission plane on the phase shift between the input and output shaft rotational displacement at different frame angles. This knowledge will provide a reference for existing shaft couplings to be evaluated and modified to optimize shaft transmission tolerances as a function of the ball groove clearances and pilot lever motion accuracy. The type of CV shaft couplings, where the axes of rotation of the shafts intersect will be investigated in this study and the errors which occur when the homokinetic-plane requirement is not satisfied will be presented and quantified. The relationship between the ball-groove contact location and the deviation from constant-velocity of the coupling (when the transmission plane is not coincident with the homokinetic plane) is the focus of this study.

1.6 Description of the Topic of each Chapter

Chapter 2 will provide the theoretical background and the development of the CV shaft coupling model. Chapter 3 explains the mathematical procedure which transforms the CV shaft coupling model into an explicit solution. Chapter 4 implements the model for various geometric configurations. A brief discussion will also be offered describing characteristics of particular interest found in the results. Chapter 5 will summarize the study and offer insight as to how this study provides essential information for the improvement of CV couplings.

CHAPTER 2
DEVELOPMENT OF THE MODEL

2.1 General discussion of approach

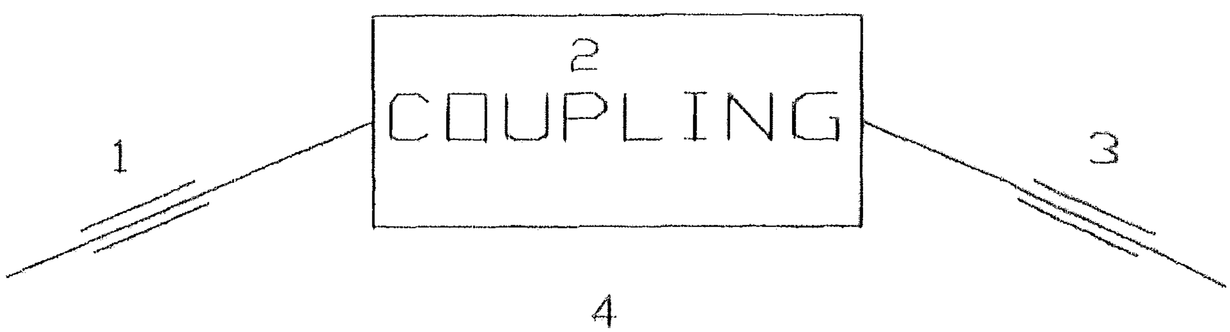

Fig. 2-1 General Black Box Coupling

A conceptual discussion of model development is presented in this chapter. The coupling model will be a multiloop system consisting exclusively of successive orthogonal revolute joints, which have been chosen as fundamental building blocks. To develop the model, a modified graph theory will be used to visualize the construction. Modified graph theory is an extension of the mechanism-categorizing, type-synthesis, technique developed by *Freudenstein* (1978). While in the mechanism type-synthesis graph theory the relationship between links through joints was specified, graphs will be used here to specify the relationships between coordinate frames fixed on the links and the base through coordinate transformations. The constraints that describe this will be individually contended with as the model is formulated. The criteria such as the degrees-of-freedom and the general principle of the homokinetic plane will be incorporated into with a general "black box" shaft coupling.

2.2 Degree-of-freedom criteria

A generalized shaft coupling is a one degree-of-freedom mechanism which will provide the first formulation. The following degree-of-freedom equation can be be utilized to implement the first constraint for the generalized shaft coupling.

$$F = -\lambda L_{ind} + \Sigma f_i \tag{2-1}$$

$$L_{ind} = j - l + 1 \tag{2-2}$$

where variables are defined such that:

F	=	degree of freedom of the system
λ	=	degree of freedom of the space
l	=	number of links in the system
j	=	number of rotations in the system
Σf_i	=	number of freedoms in the system
L_{ind}	=	number of independent closed loops

This equation will be used evaluate the shaft coupling where all the axes of rotation intersect at a single point, which justifies projecting the system onto spherical space which is a three freedoms space, $\lambda = 3$, characterized by X, Y and Z rotations. A simple shaft coupling is defined as having a single independent loop, $L_{ind} = 1$; and a single degree of freedom, $F = 1$, so that

$$1 = -3\,(1) + \Sigma f_i \tag{2-3}$$

$$4 = \Sigma f_i\,. \tag{2-4}$$

This value corresponds to the Cardan joint, which with four revolute joints, has the minimum number of freedoms possible for a shaft coupling. It is important to note that for the Cardan joint all axes of rotation of these revolute joints in series are perpendicular to their neighbors, except for the terminal joints. The terminal joints represent the rotation of the input and output shafts. This lack of symmetry of all couplings with an even number of freedoms in spherical space is the reason non-constant velocity transmission occurs. An additional degree of freedom in the system is needed to comply with the odd number of rotations requirement described by *Hunt (1973)*. Since constant velocity is desired, the freedoms of the system will be set to $\Sigma f_i = 5$. This result is valid for a double Cardan joint where the intermediate shaft is reduced to zero length. Considering a coupling with five revolute joints, eq (2-1) is evaluated as eq (2-5). Five revolute joints, whose axes intersect at a point, meets the odd number of freedoms requirement, yet represent a two degree-of-freedom system. An external device to align the homokinetic plane will account for the second degree-of-freedom.

$$-3(1) + 5 = 2 \tag{2-5}$$

To satisfy the symmetry relationship between the shafts, the axes of rotation of the joints configured about the central joint must intersect in the homokinetic plane which creates indeterminant configurations of the central joint. Indeterminate configurations occurs at some point during the articulation of the shaft coupling ,when the two neighboring revolute joints axes of rotation become collinear. The indeterminacy of the central joint can only be eliminated by locating it with an external device. Thus it is the intention of this study to locate the central joint with an external device. The additional degree of freedom will be allocated to the locating device which will specify the position of the central joint.

2.3 Application of modified graph theory

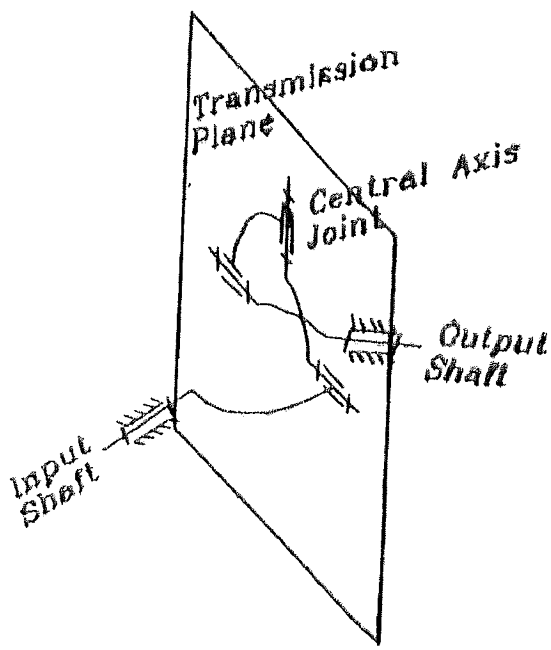

Fig. 2-2 The central axis joint in an indeterminant configuration, where its two neighboring joints axes are collinear and redundant.

To develop the coupling model, a modified graph theory will be employed since the parameters that describe the fixed frames play an important role in this construction and would be excluded with the existing graph theory. Graph theory is a method of representing mechanisms with a combination of vertices (v) and edges (e). The vertices, as points, will represent frames and the edges, as lines, will represent rotations.

The joint rotations symbolized in Fig. 2-3 can be combined by condition of

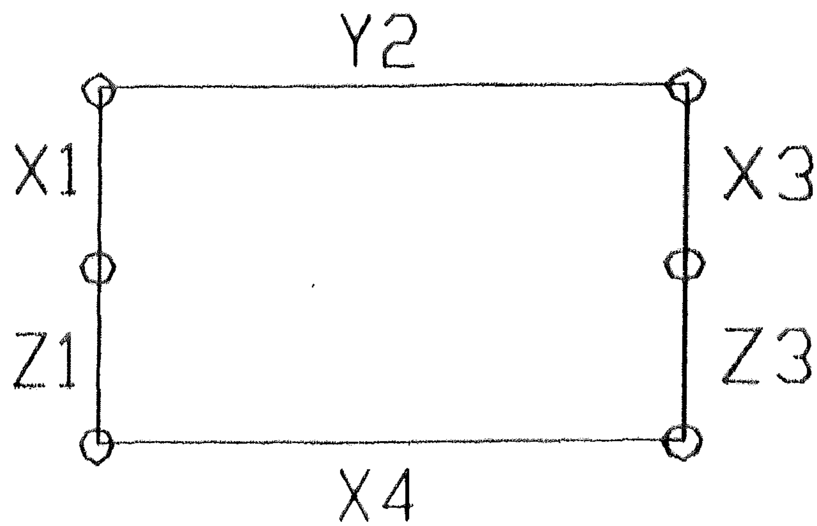

Fig. 2-3 Modified graph theory diagram of underconstrained CV coupling.

loop closure as

$$Z_1 X_1 Y_2 X_3 Z_3 X_4 = I \qquad (2\text{-}6)$$

where:

Z_1 = Input Shaft Rotation
X_1 = Input Shaft Alignment Angle
Y_2 = Rotation with axis in transmission plane
X_3 = Output Shaft Alignment Angle
Z_3 = Output Shaft Rotation
X_4 = Frame Angle

The choice of rotation axes were selected to maintain symmetry between the shafts and adhere to the common convention of shaft rotations about Z axes. By defining the frame angle as a parameter, the system satisfies the five joint freedoms constraint.

This system must be expanded to allow the location of the central joint axis to be specified. An additional relationship between the central joint axis and the fixed frame will offer a means of prescribing the orientation of the transmission plane. The central joint axis lies in the transmission plane according to the principle of the homokinetic plane. Consider expanding the central joint rotation into two separate angles about the same axis. This expansion of the system will not effect the freedoms of the system since the new rotations, Y_1 and Y_3, shown in Fig. 2-4, are redundant with the original rotation Y_2. The frame between the redundant transmission angles is located in the transmission plane. The magnitude of the rotations Y_1 and Y_3 are proportioned to define a frame located in the transmission plane so that

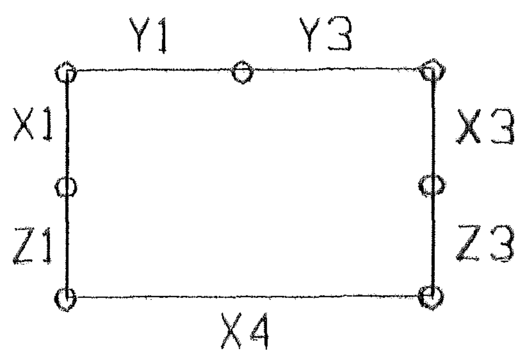

Fig. 2-4 CV coupling with frame in transmission plane.

$$Y_2 = Y_1 Y_3 \tag{2-7}$$

The frame angle will also be split into two redundant angles at this stage in the development of the model. The new frame developed between the Y_1 and Y_3 rotation will be connected to the new transmission frame by an additional rotation. This rotation between a frame in the transmission plane and the fixed frame will have its axis perpendicular to the transmission plane, and will articulate the central-joint axis about the prescribed transmission plane so that the rotation through the frame angle, which is the sum of the rotations X_{21} and X_{23}, shown in Fig. 2-5, is

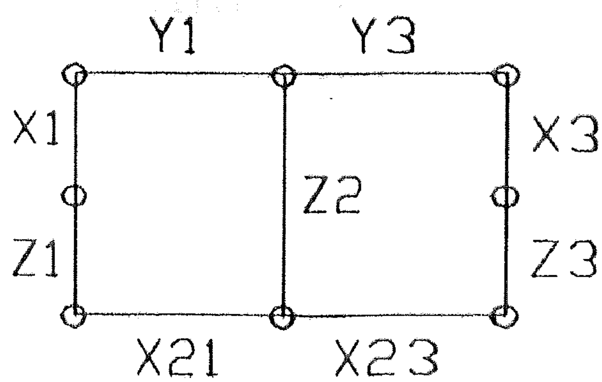

Fig. 2-5 CV Coupling with Rotation in Transmission Plane

$$X_4 = X_{21} X_{23} \quad (2\text{-}8)$$

The Z_2 transmission rotation, shown in Fig. 2-5, whose axis is perpendicular to the axes of the Y_2 and X_4, rotations, defines an axis perpendicular to the transmission plane. The transmission plane is the locus of positions of the central-joint through articulation of the coupling. Each location of the central-joint axis will be constrained about this rotation which defines the transmission plane. The transmission rotation axis can only achieve positions perpendicular to the frame angle axis in this formulation, as one single rotation is installed to locate the transmission plane about the frame angle.

By expanding the transformation specifying the ground link (frame angle) with a set of two Y-rotations, Y_{21} and Y_{23},shown in Fig. 2-6, it will be possible to evaluate all transmission plane location possibilities. By prescribing the two Y-rotations with a product equal to the identity matrix, they will not effect the original configuration. It is critical to maintain characteristics of the original system to maintain the frame angle about the X-axis. This is the final configuration which can will be developed into a mathematical model.

The mechanism can be considered as a two-loop structure, represented by the modified graph theory diagram shown in Fig 2-6, where,

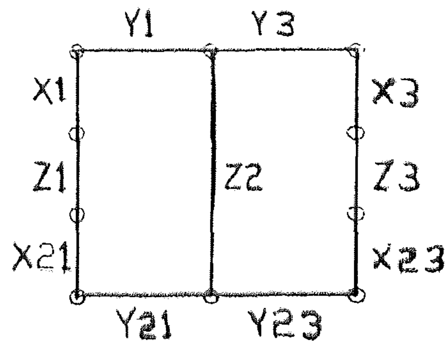

Fig. 2-6 Modified Graph Theory Diagram of Solution Model

Input Loop:

$$Z(\theta_1)X(\alpha_1)Y(\eta_1)Z(\theta_2)Y(\eta_{21})X(\alpha_{21})=I \tag{2-9}$$

Output Loop:

$$Z(\theta_3)X(\alpha_3)Y(\eta_3)Z(\theta_2)Y(\eta_{23})X(\alpha_{23})=I \tag{2-10}$$

where,

Z_1, Z_3 = Input and Output Shaft Rotations (variables)
Y_1, Y_3 = Central Axis Joint Rotations (variables)
X_1, X_3 = Outer Joints Rotations (variables)
Z_2 = Rotation in Transmission Plane (variables)
X_{21}, Y_{21} = Input Shaft Frame Rotations (parameters)
X_{23}, Y_{23} = Output Shaft Frame Rotations (parameters)

These rotations will be thoroughly explained in the mathematical model that follows. To confirm the validity of the modifications the model, the degree of freedom equation will be used. For this model must maintain 1 degree of freedom in the system, $F = 1$, through two independent loops, $L_{ind} = 2$. The number of freedoms is predicted to be $\Sigma f_i = 7$. The number of freedoms corresponds to the number of variable rotations in the system which confirms this system is valid.

CHAPTER 3
DESCRIPTION OF MATHEMATICAL MODEL

3.1 General discussion of mathematical techniques

This model is developed on the premise that the all the axes of rotation intersect at a single point in space, which allows the model to be projected onto spherical space. This configuration is particularly relevant to the ball-groove CV joint as the balls of the central-joint maintain a circular orbit in the transmission plane. Although the central-joint of a CV joint is ideally constained to the homokinetic plane, it is not particular to the instantaneous radius, only to the instantaneous angular position. From this principle the central-joint need not perform a circular orbit in the transmission plane. This model will assume a circular orbit which maintains the exact instantaneous angular position. This provision simplifies the model, yet does not effect the input-output relationship. The static forces and torques on the balls in the ball-grooves of a CV joint was accomplished by *Bellomo* (1975), which excludes all non-constant-velocity configurations due to mechanical tolerances and wear, yet confirms the circular orbit of the central-axis joint.

The term "I" denotes the identity transformation and for spherical space represents a diagonalized 3x3 unity matrix. Each of the rotational transformations are 3-dimensional proper orthogonal rotation matrices in this solution scheme, which can be denoted by

$$Z(\theta) = \begin{bmatrix} C\theta & -S\theta & 0 \\ S\theta & C\theta & 0 \\ 0 & 0 & 1 \end{bmatrix} \qquad Y(\eta) = \begin{bmatrix} C\eta & 0 & S\eta \\ 0 & 1 & 0 \\ -S\eta & 0 & C\eta \end{bmatrix} \qquad X(\alpha) = \begin{bmatrix} 1 & 0 & 0 \\ 0 & C\alpha & -S\alpha \\ 0 & S\alpha & C\alpha \end{bmatrix} \tag{3-1}$$

using the notation,

$$C\theta = \cos(\theta), \quad S\theta = \sin(\theta), \quad and \quad T\theta = \tan(\theta).$$

3.2 Application of mathematical techniques to model

The rotational transformations are concatenated in a double-closed chain to represent the CV shaft coupling model. This is achieved using a closed form solution method. In this context "closed form" means a solution method based on analytic expressions, such that non-recursive calculations suffice to arrive at a solution (*Craig* 1986). Double-closed chain implies the use of loop closure for a system of rotations which achieve closure with two interdependent loops. Each of the elements of the matrix product of a closed chain represent a structure equation descriptive of the coordinate transformations in that loop, which comes to n^2 equations for n-space. The result is a constraint on the allowable values of the joint rotations in the chain, which maintain the closure of the chain (*McCarthy* 1990).

The input-output rotational displacement relationship can be solved from the two closed loop equations. The relationship between the input shaft and the transmission rotational displacement is solved in the first loop. The corresponding transmission rotational displacement is applied to solve for the output-shaft rotational displacement in the second loop. The total system at this point has one degree of freedom with four parameters to describe the locations of the rotations of links connected to the fixed-frame. As was previously mentioned, the Y-axis rotations are equally opposite which reduces the fixed frame description to three parameters. The single degree of freedom will be the rotation of the input shaft to obtain the corresponding output shaft rotational displacement.

To maintain the customary convention of the input and output shaft axes as Z-axes pointing outward, some modifications will be employed. The rotations in the transmission plane for each of the loops will be supplementary. The necessary changes can be seen in Fig. 3-1. The θ_2 and θ_3 values in the output loop will have signs opposite from the sense of the input loop. The α_1 and α_3 values are now the supplement of the frame angle also called the driveline angular offset. These modifications produce a genuinely simplified model as both sides of the shaft coupling are now modeled identically.

This model maintains essential characteristics of the original configuration while incorporating the transmission plane locating device. The first closed loop of rotations relating the input shaft to the transmission plane takes the form ZXYZYX = I. The second closed loop of rotations relating the transmission plane to the output shaft and takes the identical form ZXYZYX = I.

The model is represented in Fig. 3-1 as successive coordinate frames. These coordinate frames are characterized by the rotation at that location in the closed loop chain. This figure makes the mathematical model easier to understand and visualize.

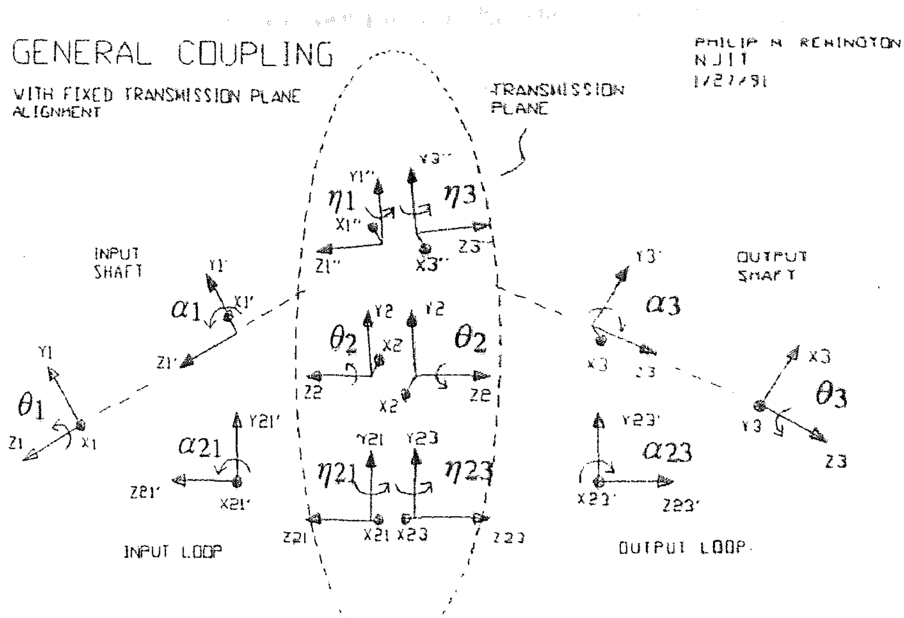

Fig. 3-1 General Coupling with Fixed Transmission Plane.

The loop equations are

Input Loop:

$$Z(\theta_1)X(\alpha_1)Y(\eta_1)Z(\theta_2)Y(\eta_{21})X(\alpha_{21})=I$$

Output Loop:

$$Z(\theta_3)X(\alpha_3)Y(\eta_3)Z(\theta_2)Y(\eta_{23})X(\alpha_{23})=I$$

where

$Z_1(\theta_1), Z_3(\theta_3)$ = Input and Output Shaft Rotations (variables)

$Y_1(\eta_1), Y_3(\eta_3)$ = Central- Axis Joint Rotations (variables)

$X_1(\alpha_1), X_3(\alpha_3)$ = Outer Joint Rotations (variables)

$Z_2(\theta_2)$ = Rotation in Transmission Plane (variables)

$X_{21}(\alpha_{21}), Y_{21}(\eta_{21})$ = Input Shaft Frame Dimensions (parameters)

$X_{23}(\alpha_{23}), Y_{23}(\eta_{23})$ = Output Shaft Frame Dimensions (parameters)

The fixed frame is parameterized by the driveline offset angles, α_{21} and α_{23} for the input and output loops, respectively. The corresponding fixed frame angles, η_{21} and η_{23} will occur about the axis perpendicular to the driveline offset angles in the transmission plane. The input-shaft rotation is input-variable angle θ_1 and the output shaft rotation is output-variable angle θ_3. These loops both have the same transmission rotation through intermediate variable angle θ_2, in the transmission plane which connects them. The sign of the transmission rotation will be opposite from one loop to the other for convienient notation. Let it be noted that the Z_2-transmission rotation is the rotation of the locating device which constrains the Y-rotation, central-joint axis to the transmission plane.

The input loop is evaluated for function $\Theta_2 = \Phi(\theta_1,\eta_{21},\alpha_{21})$, the transmission rotation, by expanding the rotation transformations in the form,

$$X(\alpha_1)Y(\eta_1)Z(\theta_2)= (Y(\eta_{21})X(\alpha_{21})Z(\theta_1))^T \tag{3-2}$$

to obtain intermediate variable Θ_2, element (1,2) is divided by (1,1),

$$T_{\theta_2}=\frac{-S_{\theta_1}C_{\alpha_{21}}}{C_{\theta_1}C_{\eta_{21}}+S_{\theta_1}S_{\eta_{21}}S_{\alpha_{21}}}. \tag{3-3}$$

The output loop is evaluated for function $\Theta_3 = \Phi(\Theta_2,\eta_{23},\alpha_{23})$ by expanding the equation in the form,

$$Z(\theta_3)X(\alpha_3)Y(\eta_3)= (Z(\Theta_2)Y(\eta_{23})X(\alpha_{23}))^T \tag{3-4}$$

and to obtain output variable Θ_3, element (1,2) is divided by (2,2),

$$T_{\Theta_3}=\frac{-S_{\Theta_2}C_{\eta_{23}}}{C_{\theta_2}C_{\alpha_{23}}+S_{\Theta_2}S_{\eta_{23}}S_{\alpha_{23}}}. \tag{3-5}$$

It is essential to take make provisions for quadrant changes, which the general arctangent function does not, in refining the solution. The function, ATAN2(sin(θ),cos(θ)), a FORTRAN notation, can be incorporated into the solution for both Θ_2 and Θ_3 to obtain the correct quadrants in the solution.

$$\Theta_2 = \text{ATAN2}(-S_{\theta 1}C_{\alpha 21}\ ,\ C_{\theta 1}C_{\eta 21} + S_{\theta 1}S_{\eta 21}S_{\alpha 21}) \tag{3-6}$$

$$\Theta_3 = \text{ATAN2}(-S_{\Theta 2}C_{\eta 23}\ ,\ C_{\Theta 2}C_{\alpha 23} + S_{\Theta 2}S_{\eta 23}S_{\alpha 23}) \tag{3-7}$$

These equations together make up the generalized input/output relationship for the CV coupling including the configurations where constant-velocity constraints are not satisfied. By substituting eq (3-6) into eq (3-7) can be obtained the generalized coupling input/output equation,

$$\Theta_3 = \text{ATAN2}(\Psi_1 S_{\theta 1}\ ,\ \Psi_2 C_{\theta 1} + \Psi_3 S_{\theta 1}) \tag{3-8}$$

where

$$\Psi_1 = -C_{\alpha 21}C_{\eta 23}$$

$$\Psi_2 = C_{\alpha 23}C_{\eta 21}$$

$$\Psi_3 = S_{\eta 21}S_{\alpha 21}C_{\alpha 23} + C_{\alpha 21}S_{\alpha 23}S_{\eta 23}$$

The focus of this study is the rotational phase shift between the input and output shaft rotational displacements for specified configurations so the following analysis will deal with the deviation,

$$\Theta_{dev} = -\Theta_3(\theta_1, \eta_{21}, \alpha_{21}, \eta_{23}, \alpha_{23}) - \theta_1 \tag{3-9}$$

3.3 Refinement of mathematical model

A scheme to make the solution more amenable will simplify the variable angles into three functions of the original variables and the input shaft rotation. The new variables will be defined as the frame angle and two orthogonal locating-device transmission angles, which are illustrated in Fig. 3-2. The provision that angle $\eta_{dev}=\eta_{21}=\eta_{23}$ is incorporated to add simplicity to the system, without loss of generality, regarding the shaft couping. This provision reduces the five degrees of freedom system to four, although these two original variables were previously defined as equal. The frame angle used throughout the development can now be taken to full advantage by the transformation $X_4 = X_{21}X_{23}$ which represents rotation through the angle $\alpha_4 = \alpha_{21}+\alpha_{23}$. Again the modification discussed and illustrated in the first section of this chapter leads to the use of a supplementary value. The angle, α_4 is now redefined as the driveline offset angle, which is the supplement of the frame angle illustrated in Fig.3-2. The frame angle is the angle between the shafts about an axis perpendicular to both shafts. The frame angle between the input and output shafts is angle $\alpha_{frame} = \pi-(\alpha_{21}+\alpha_{23}) = \pi-\alpha_4$, which uses the property that the frame angle is the supplement of the driveline offset. For this system the homokinetic plane is maintained when $\alpha_{21} = -\alpha_{23}$ and the transmission plane under the influence of the alpha transmission angle deviates from the homokinetic plane by the difference between these angles now defined as angle $\alpha_{dev}=(\alpha_{21}-\alpha_{23})/2$.

These manipulations produce three desired functions which define angles α_{21}, α_{23}, η_{21} and η_{23} in terms of angles η_{dev}, α_{dev} and α_{frame}.

$$\eta_{21} = \eta_{23} = \eta_{dev}. \tag{3-10}$$

$$\alpha_{21} = (\pi-\alpha_{frame})/2+\alpha_{dev} \tag{3-11}$$

$$\alpha_{23} = (\pi-\alpha_{frame})/2-\alpha_{dev} \tag{3-12}$$

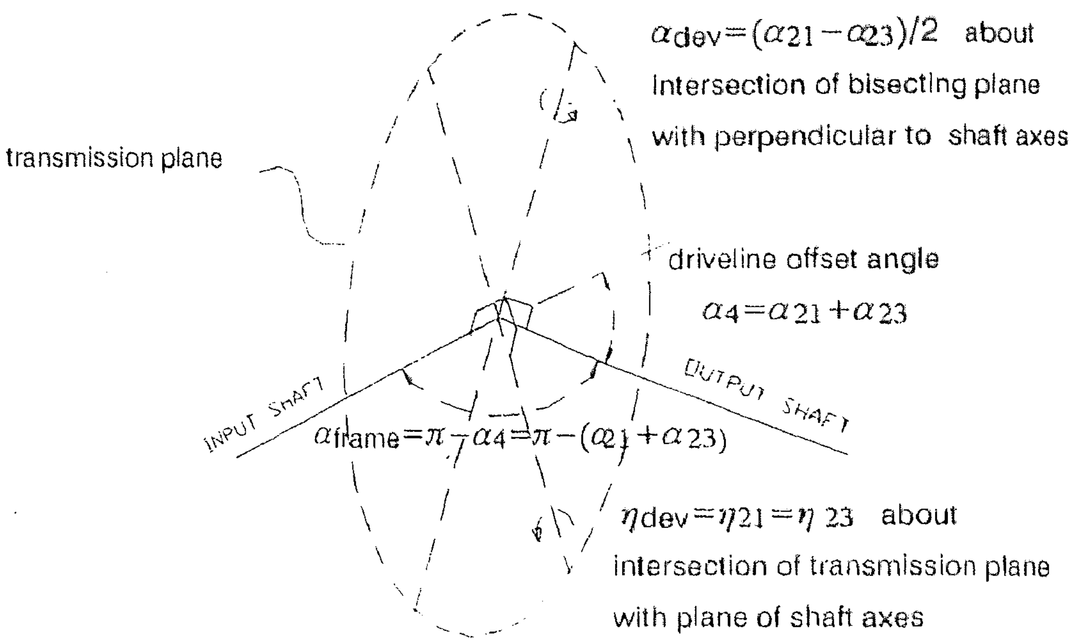

Fig. 3-2 New variables for amenable solution

Utilizing these new variables with some algebraic and trigonometric manipulation a more amenable solution will be developed. This is a concise generalized solution for the coupling input/output equation for specified transmission planes.

$$\Theta_{dev} = -\mathrm{ATAN2}(\Psi_1 S_{\theta 1}, \Psi_2 C_{\theta 1} + \Psi_3 S_{\theta 1}) - \theta_1 \qquad (3\text{-}13)$$

$$\Psi_1 = S(\alpha_{dev} - \alpha_{frame}/2)$$

$$\Psi_2 = S(\alpha_{dev} + \alpha_{frame}/2)$$

$$\Psi_3 = T_{\eta dev} S_{\alpha\,frame}$$

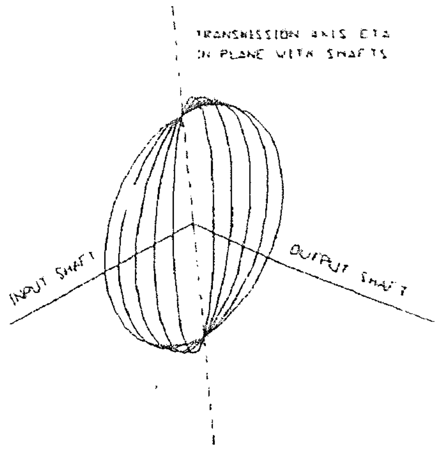

Fig. 3 - 3 Locating Scheme for Eta Transmission Axis.

The frame angle is comprised of a single X-rotation about an axis perpendicular to both the input and output shafts. The transmission angle α_{dev} occurs about the same axis and describes the angle between the transmission plane and the bisecting plane. The transmission angle η_{dev} occurs about an axis in both the transmission plane, determined by the transmission angle α_{dev}, and the plane that contains both shafts. These two angles give the ability to locate the transmission in any orientation desired.

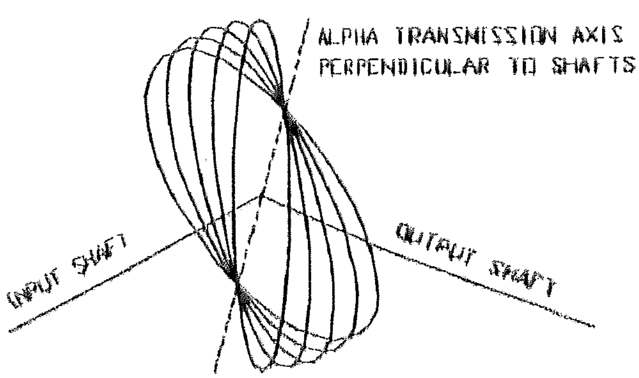

Fig. 3 - 4 Locating Scheme for Alpha Transmission Axis.

The transmission angle α_{dev} defines the location of the transmission plane with respect to the homokinetic plane about an axis perpendicular to both shafts. The transmission axis η_{dev} is located at the intersection of transmission plane located by the angle α_{dev} and the plane that contains both shafts. The angle η_{dev} and the angle α_{dev} are parts of the fixed frame that give the ability to achieve all possible transmission plane orientations.

CHAPTER 4
RESULTS AND DISCUSSION

4.1 Discussion of Amenable Variable Scheme

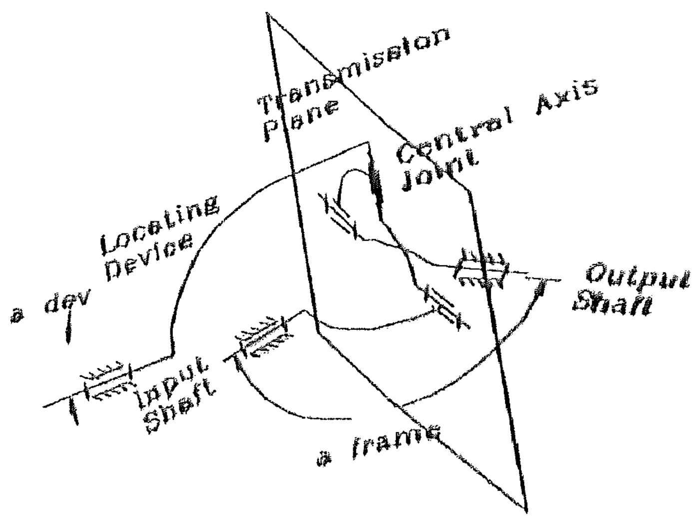

Fig. 4 - 1 Alpha transmission angle about axis perpendicular to both shafts

The transmission angles α_{dev} and η_{dev} provide a means of referencing the angular phase shift between the input and output shafts to the location of the transmission plane. With the new variables developed in the previous chapter, this shows to be a more amenable scheme, as this equation shows.

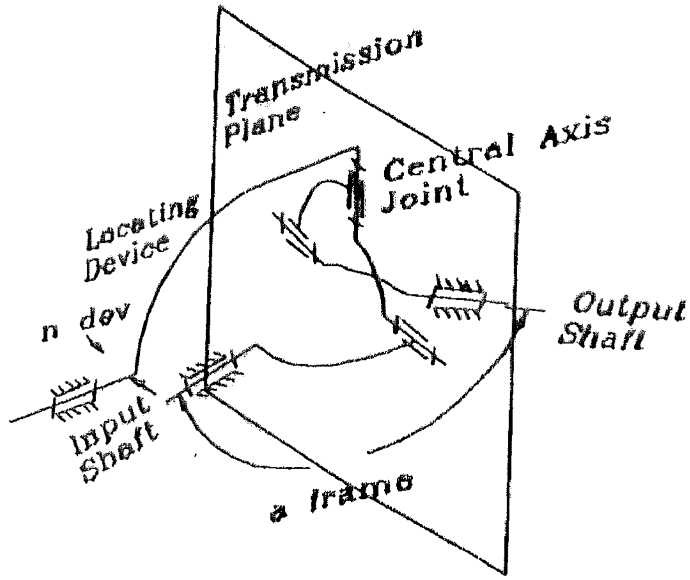

Fig. 4 - 2 Eta transmission angle about axis in plane with both shafts

$$\Theta_{\text{dev}} = \text{ATAN2}(\Psi_1 S_{\theta 1}, \Psi_2 C_{\theta 1} - \Psi_3 S_{\theta 1}) - \theta_1 \qquad (4\text{-}1)$$

$$\Psi_1 = C((\alpha_{\text{frame}} - \alpha_{\text{dev}})/2)$$

$$\Psi_2 = C((\alpha_{\text{frame}} + \alpha_{\text{dev}})/2)$$

$$\Psi_3 = T_{\eta\text{dev}} S_{\alpha\text{ frame}}$$

4.2 Presentation of Solutions for Trial Parameters

It is important to note each of the deviation parameters in this model are referenced the homokinetic plane. The frame angle determines the location of the homokinetic plane, implicitly. This allows the deviation of the transmission plane from the homokinetic plane to be controlled exclusively by the angles α_{dev} and η_{dev}.

The deviation through a complete articulation of the coupling for the case with angle $\eta_{dev} = 0°$ is shown in Figures 4-3,4-4.

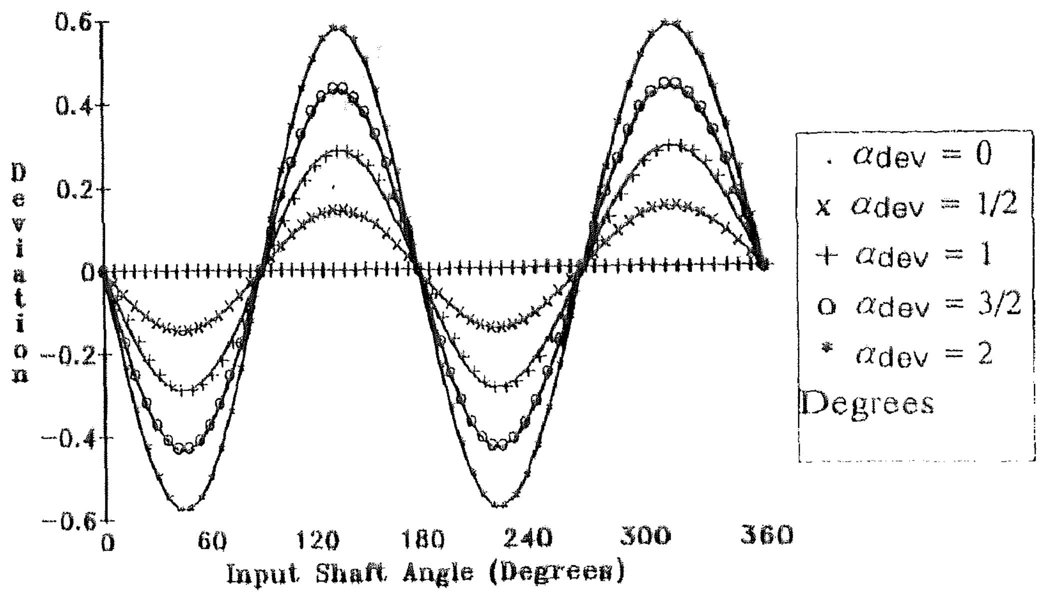

Fig. 4 - 3 Input/Output shaft deviation with α_{frame} = 120 degrees for various α_{dev} values.

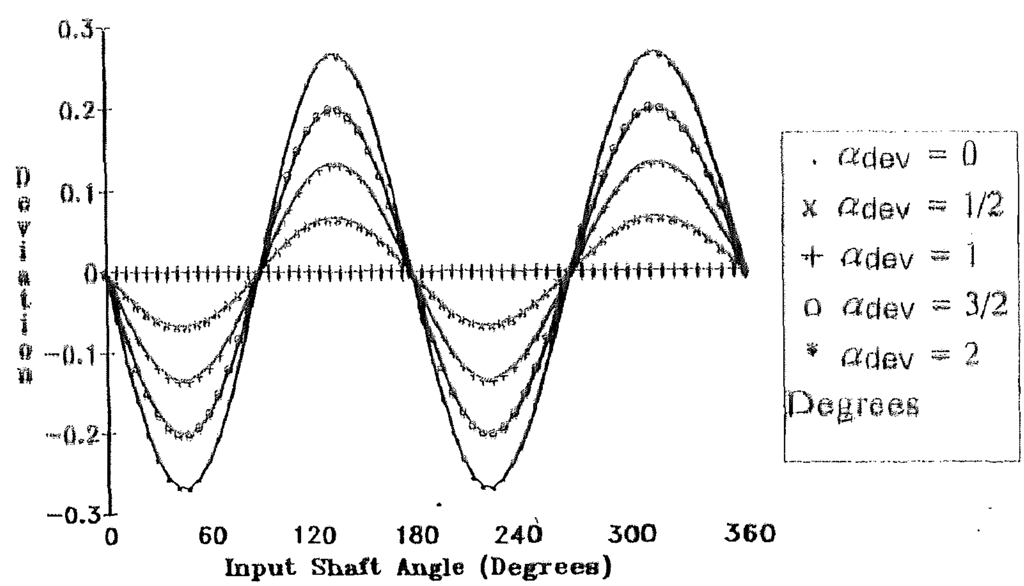

Fig. 4 - 4 Input/Output shaft deviation with α_{frame} = 150 degrees for various α_{dev} values.

The deviation through a complete articulation of the coupling for the case with $\alpha_{dev} = 0°$ is shown in Figures 4-5,4-6.

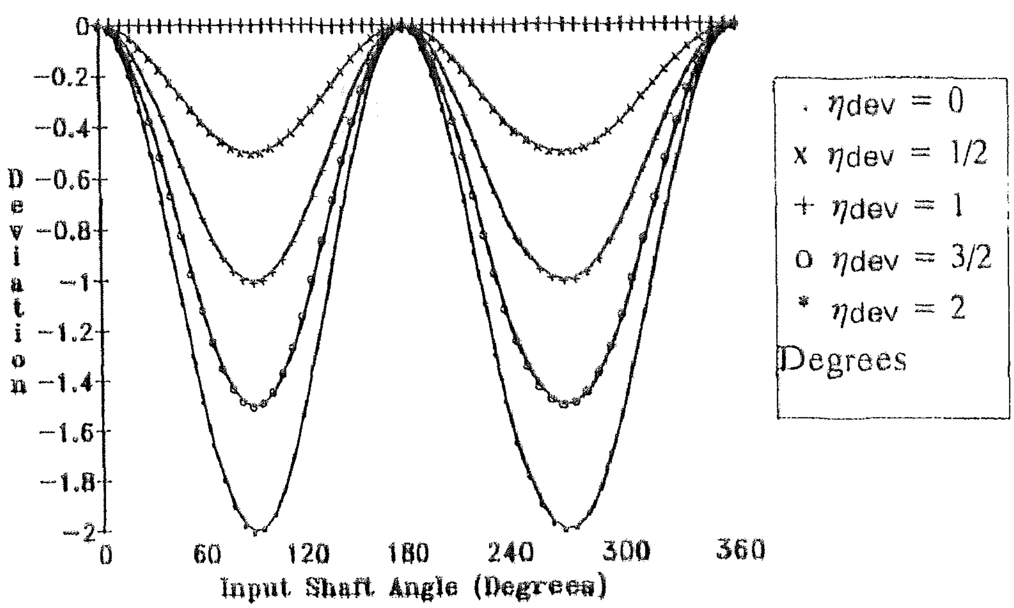

Fig. 4 - 5 Input/Output shaft deviation with α_{frame} = 120 degrees for various η_{dev} values.

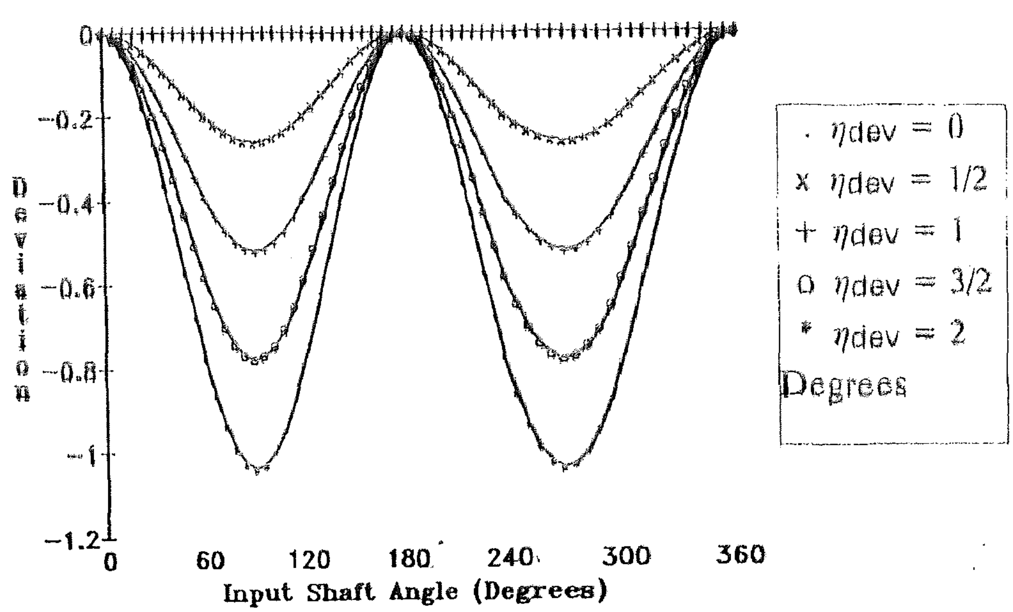

Fig. 4 - 6 Input/Output shaft deviation with α_{frame} = 150 degrees for various η_{dev} values.

A general set of solutions incorporate combinations of the transmission angles α_{dev} and η_{dev} for frame angles, $\alpha_{frame} = 120°$ and $150°$ as shown in Figures 4-7,4-8.

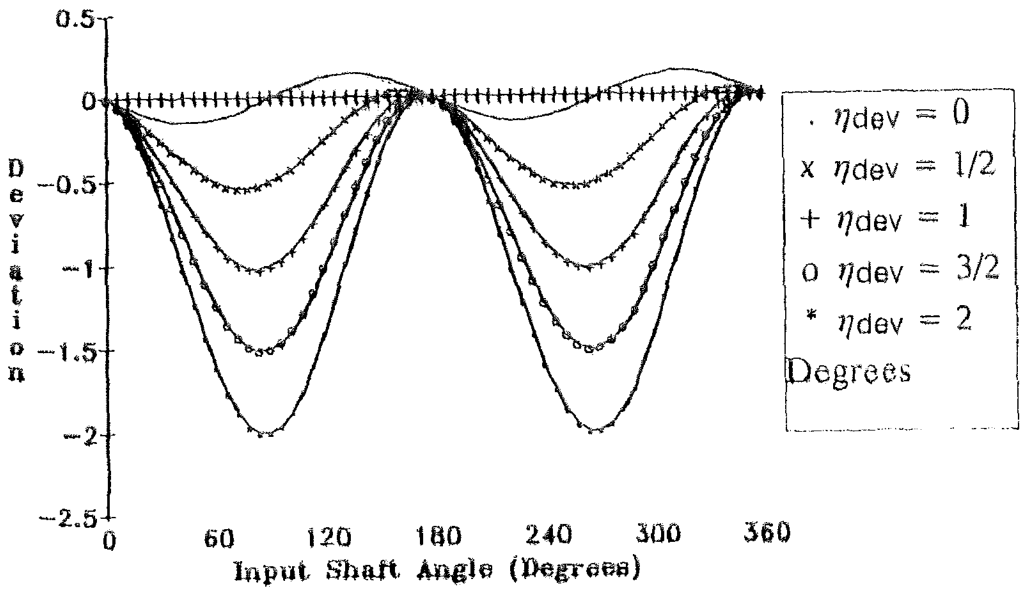

Fig. 4 - 7 Input/Output shaft deviation with α_{frame} = 120 degrees and α_{dev} = 1/2 degree for various η_{dev} values.

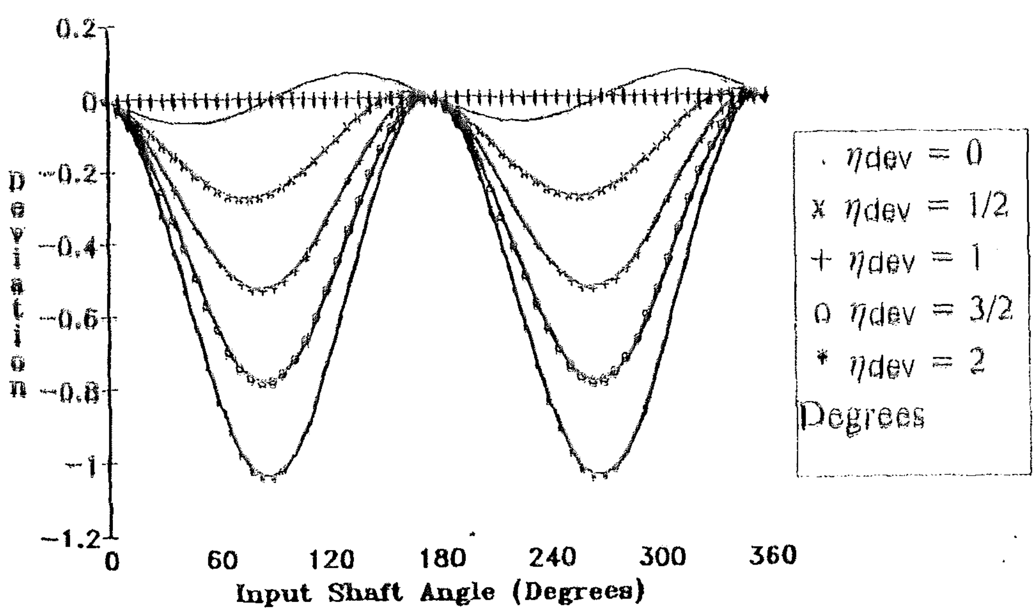

Fig. 4 - 8 Input/Output shaft deviation with α_{frame} = 150 degrees and α_{dev} = 1/2 degree for various η_{dev} values.

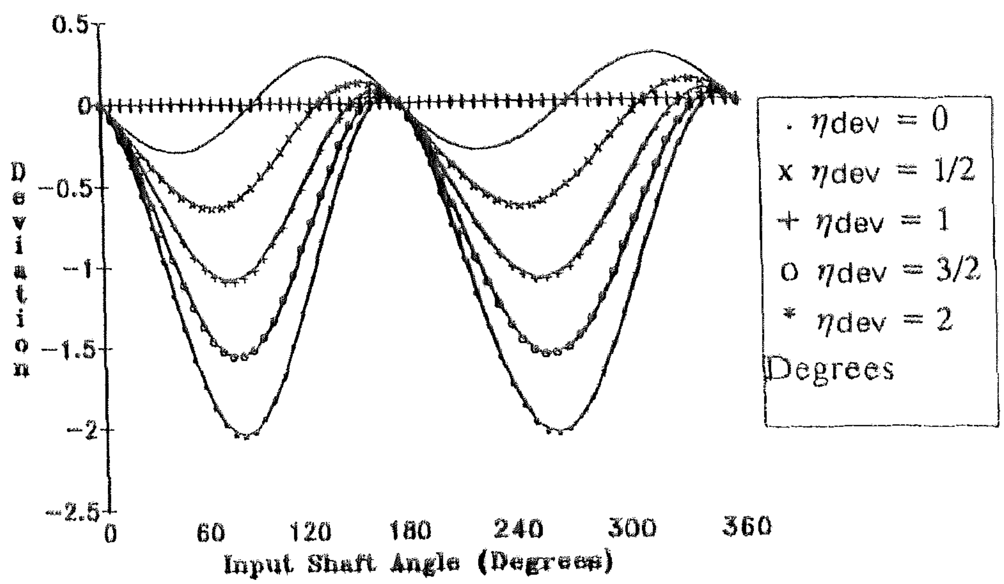

Fig. 4 - 9 Input/Output shaft deviation with α_{frame} = 120 degrees and α_{dev} = 1 degree for various η_{dev} values.

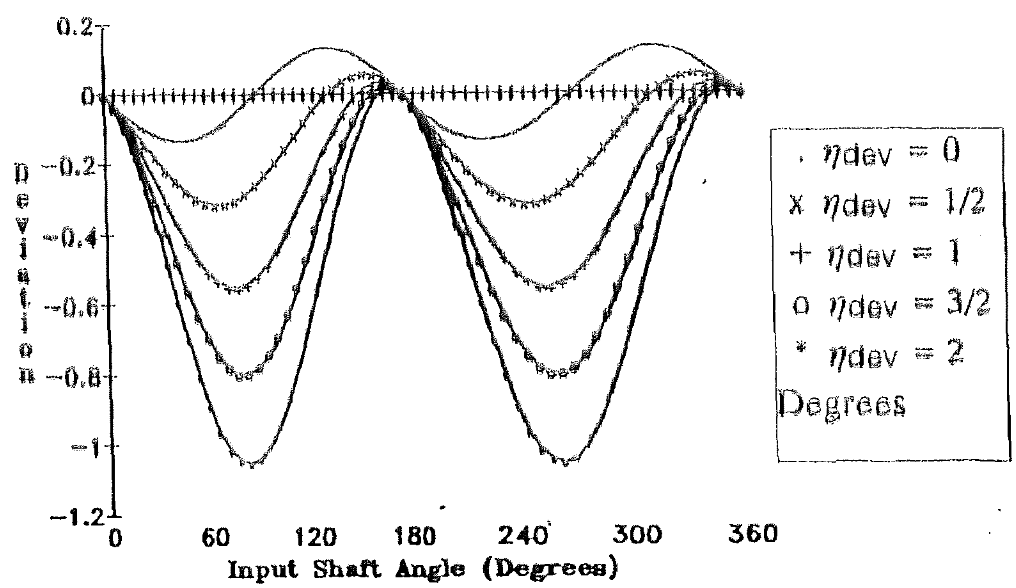

Fig. 4 - 10 Input/Output shaft deviation with α_{frame} = 120 degrees and α_{dev} =3/2 degree for various η_{dev} values.

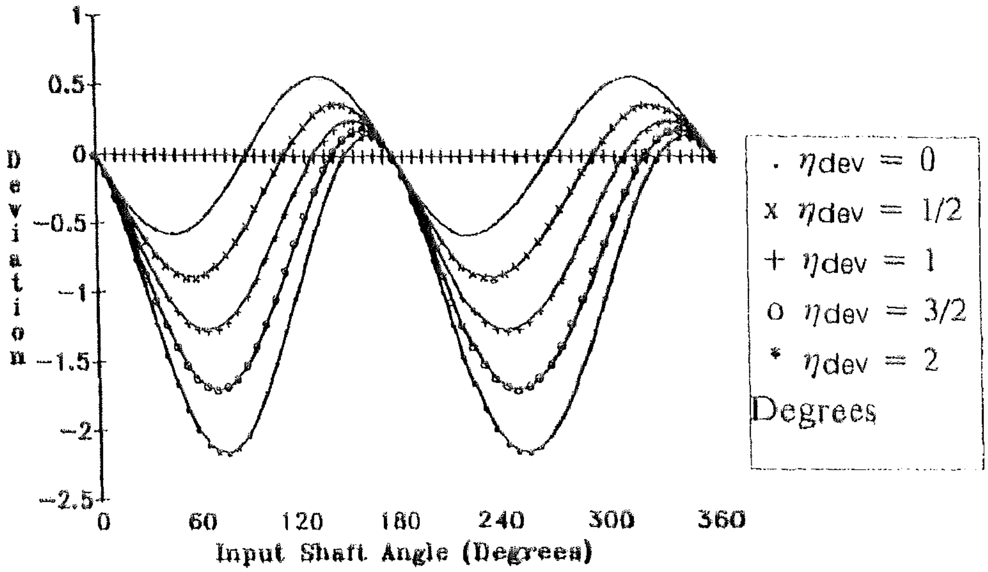

Fig. 4 - 11 Input/Output shaft deviation with α_{frame} = 120 degrees and α_{dev} =2 degree for various η_{dev} values.

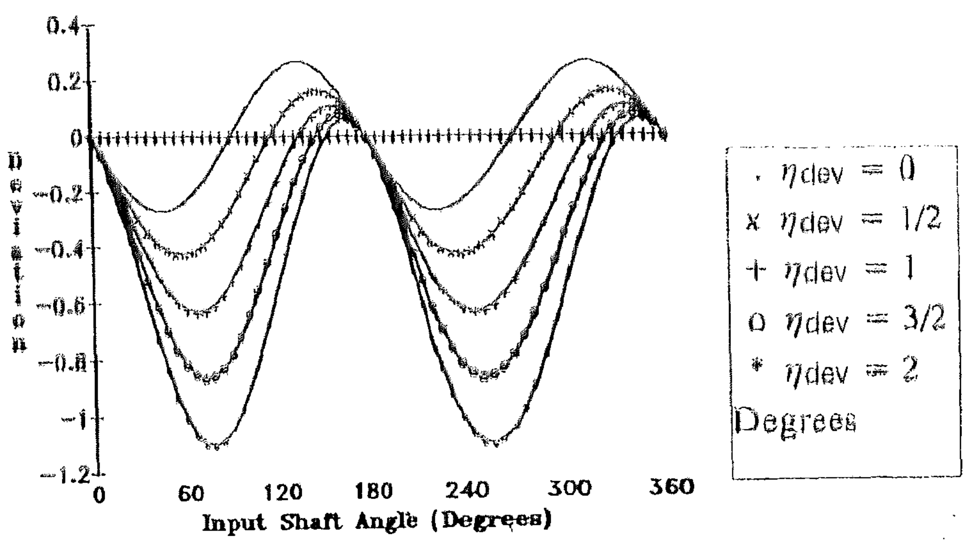

Fig. 4 - 12 Input/Output shaft deviation with α_{frame} = 150 degrees and α_{dev} =2 degree for various η_{dev} values.

4.3 Discussion of Results

The CV coupling deviation solution provides a complete relationship between the input and output shaft rotations for all possible configurations of the transmission plane. It is essential to delineate the effects α_{dev} and η_{dev}, on the input/output relationship throughout various frame angles. These two angles give absolute control over the deviation of the transmission plane with respect to the homokinetic plane. The effects of these angles can be described by grouping the orientations of the central-axis joint into quadrants.

These quadrants represent sub-sets of all possible central-axis joint locations. The quadrants are characterized by the quarter-spaces whose boundaries are central-axis joint locations which produce zero deviation between the input and output shafts. These boundaries correspond to the central-axis joint located in the homokinetic plane or the plane that contains both shafts. As either of these boundaries are crossed by the central-axis joint the deviation between the input and output shafts will switch signs. These ideas help the designer get a quick idea of the general effects of the location of the central-axis joint on the input/output relationship. The use of these quadrants will be elaborated upon, as this concept will assist in the discussion of the two deviation angle's effects upon the input/output relationship.

The α_{dev} deviation angle, when it is the only deviation of the transmission plane from the homokinetic plane, will send the central-axis joint through all four quadrants. This will assure the input/output relationship changing signs four times for one full rotation of the input shaft. The α_{dev} deviation angle has less effect on the input/output relationship per degree of deviation then does the η_{dev} deviation angle, although it is the most volatile with respect to the frame angle. The implicit locating of the homokinetic plane at one-half the frame angle directly effects the reference frame of the α_{dev}. The α_{frame} axis coincides with the α_{dev} axis which shows the direct

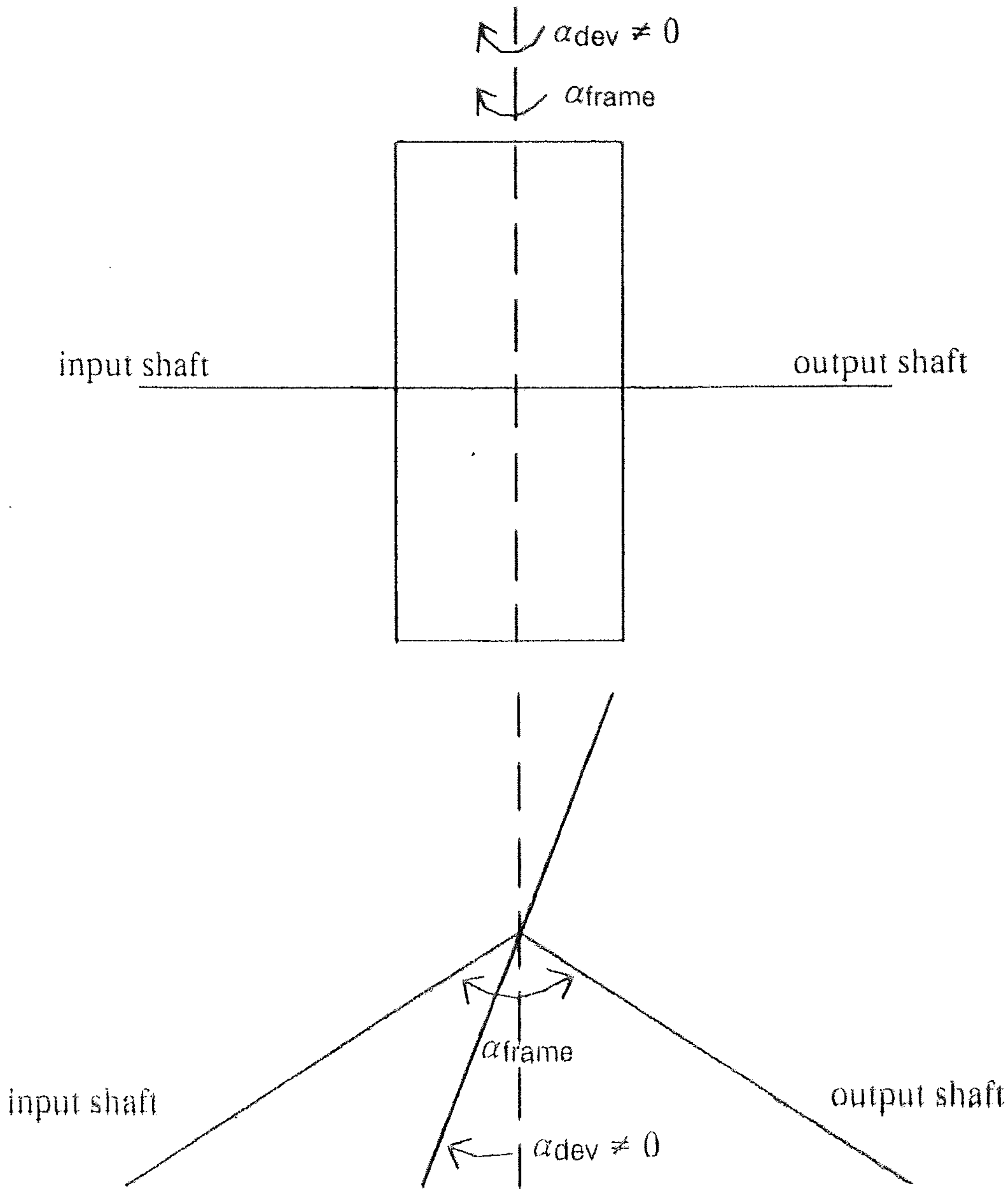

Fig. 4-13 Views of α_{dev} to destinguish the transmission plane passing through four quadrants

correlation between the α_{frame} angle and the reference frame for the α_{dev} angle. This deviation angle is the angle of greatest concern to designers as this angle contends with the axis that requires the most modification for a given change in the α_{frame} angle. The α_{dev} reference changes by one-half the change in the frame angle as it is referenced from the homokinetic plane.

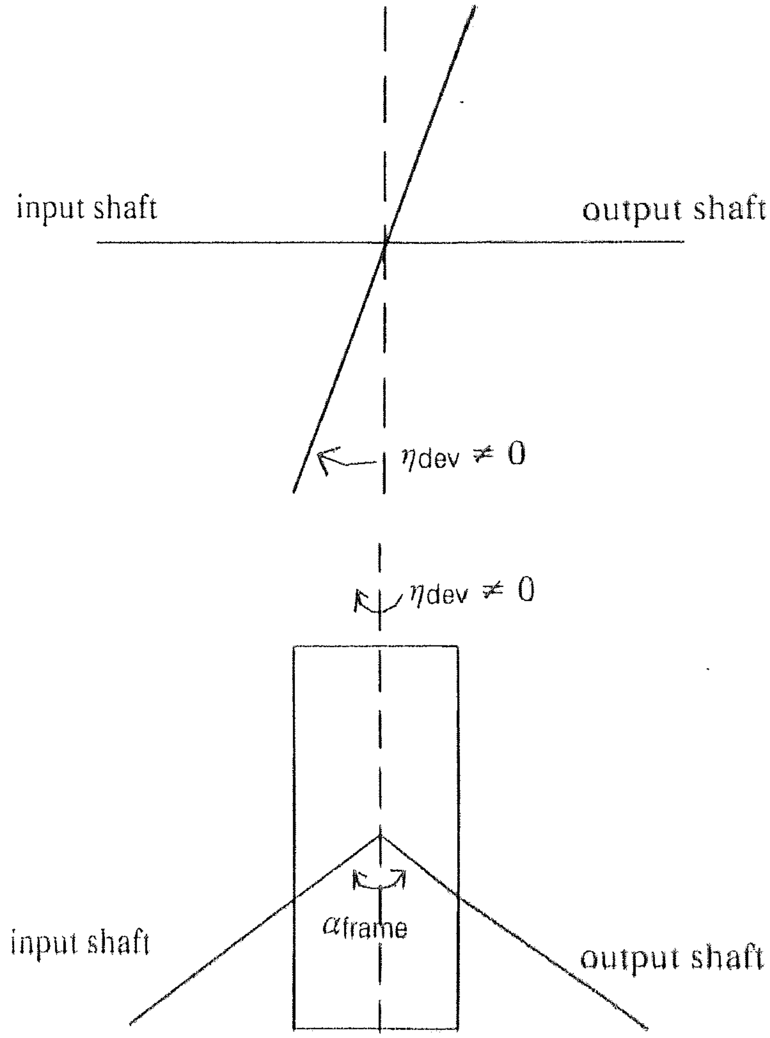

Fig. 4-14 Views of η_{dev} to destinguish the transmission plane passing through two quadrants

The η_{dev} deviation angle rotates about the axis in the transmission plane which is in the plane with both shafts. When this is the only angle of deviation the central-axis joint will pass through two quadrants of the same sign. The location of the η_{dev} axis when α_{dev} is zero is the line touching all four quadrants. By passing through this line twice the input/output relationship will maintain the same sign. The η_{dev} deviation angle has a greater effect on the input/output relationship per degree of deviation from the homokinetic plane yet, is nearly independent of the positioning of the locating device. The η_{dev} deviation axis is orthogonal to the axis of the frame angle and thus the η_{dev} reference is ideally unchanged by the bisecting angle variations.

The α_{dev} deviation angle, most dependent on the locating device, occurs about an axis perpendicular to both shafts. The α_{frame} angle rotates about the same axis as the α_{dev} angle. It should be noted that the locating of the homokinetic plane is at one-half the α_{frame} angle and in the plane with both shafts, so the α_{dev} angle as it is referenced to the homokinetic plane is most affected by the locating device. The variation in the position of the homokinetic plane about this axis during variations in the α_{frame} angle, although implicitly defined in the solution, must be considered carefully. Although the locating devices in primarily positioning the transmission plane to accommodate the new frame angles, the input/output relationship may still develop deviation by the η_{dev} angle.

The input/output relationship, Θ_{dev} for one rotation of the input shaft, passes through four quadrant boundaries when α_{dev} is non-zero. This implies the Θ_{dev} value will switch signs four times during one rotation of the input shaft. These solutions are double frequency periodic functions which are symmetric about zero when η_{dev} is zero. The larger the driveline offset angle the sharper the change and the larger the amplitude of the Θ_{dev} deviation values. The η_{dev} also produces a double frequency periodic function, although the Θ_{dev} value does not change signs. At the small deviation angles that can be attributed to tolerances and wear, the solutions appear to be sinusoidal. This is not completely true as extreme deviation angles and frame angles will show an interesting phenominon.

This phenominon becomes noticable for large deviation angles becomes particularly relevant when the central-axis joint is approaching or departing from a boundary. Note the two sides of the coupling, about the transmission plane, can be viewed as identical mechanisms. As the central axis joint approaches a boundary the Θ_{dev} values become smaller. This reducing of the Θ_{dev} value can be attributed to motions in the mechanism on each identical side of the mechanism. If the output side of the mechanism is closer to the boundary configuration then the input side, a sharp change in the Θ_{dev} value will occur. This occurs when the Θ_{dev} is appraoching zero from any quadrant. These function characteristics provide additional insight into the more volatile central-axis joint locations.

Although the amplitude of the Θ_{dev} deviation is small under the influence of the α_{dev} deviation angle, the locating device is most likely to produce greater errors about the α_{dev} deviation axis. The locating device is most apt to produce errors about this axis due to the previously discussed dependence on the α_{frame}. The small η_{dev}, when α_{dev} is non-zero, makes a considerable change in the amplitude and phase of the Θ_{dev} angle. This finding localizes the most volatile central-axis joint locations and attributes the error in the CV coupling to specific characteristics of the locating device.

The η_{dev} deviation angle produces much larger magnitudes in the Θ_{dev} deviation angle for a given cycle. The η_{dev} angle produces Θ_{dev} deviations 90° out of phase from what the α_{dev} angle produces. The general shape of the corresponding input/output relationships are quite similar between the two transmission plane deviation angles. The η_{dev} deviation axis although generally less dependent on the locating device does produce a considerably larger amplitude in the input/output relationship.

The most concerning variations in the input/output relationship occur when the two deviation angles are both non-zero. The slightest addition of the η_{dev} to the α_{dev} can change the phase and increase the amplitude amplitude. The mechanical tolerances in the locating device of a CV coupling should take into account the volatility of the η_{dev} as it can have grave effects at very minute values. As the locating device is generally concerned with positioning of the transmission plane about the axis of the frame angle, perhaps additional concern should be made to accomodate the strong influence of the η_{dev} value.

CHAPTER 5
CONCLUSION

The CV shaft coupling deviation solution provides a complete relationship between the input and output shaft rotations for all possible configurations of the transmission plane. The intent of this study is to give the designer needed insight into the relationship between the transmission plane and the deviation between the input and output shaft rotational displacements. The two deviation angles, α_{dev} and η_{dev} give absolute specification of the location of the transmission plane.

The possible central-joint axis locations are grouped into four quarter spaces. The quarter spaces are separated by the plane containing both shafts and the homokinetic plane. When the central-joint axis passes a quarter space boundary, the input/output relationship, Θ_{dev} will switch signs. This implies, if the input shaft rotation leads the output shaft rotation, then it will lag or visa-versa. As the central-joint axis moves deeper into a quarter-space the lead/lag magnitude will become larger.

The η_{dev} deviation angle per degree has a greater effect on the input/output relationship then does the α_{dev} deviation angle. The η_{dev} deviation axis is orthogonal to the axis of the frame angle and thus the η_{dev} reference angle is unchanged by the bisecting angle variations. The central-joint axis only passes through two quarter spaces under the influence of η_{dev}. By remaining in a single quarter space for 180°

the central-axis joint will reach much deeper and allow the lead/lag magnitudes to become exceedingly large. The axis of the deviation angle, η_{dev} is orthogonal to the axis of the frame angle, which shows that the deviation angle, η_{dev} is least likely to be have errors due to the variations in the frame angle. These changes in the frame angle correspond to changes in the transmission plane locating device, ideally of one-half the frame angle.

The α_{dev} deviation angle, occurs about an axis perpendicular to both shafts. The α_{frame} angle rotates about the same axis as the α_{dev} angle. The location of the homokinetic plane is at one-half the α_{frame} angle, so the α_{dev} angle as it is referenced to the homokinetic plane is most affected by the transmission plane locating device. The variation in the position of the homokinetic plane about this axis during variations in the α_{frame} angle, although implicitly defined in the solution, must be considered carefully.

The central-joint axis for one rotation of the input shaft, passes through four quarter spaces boundaries when the α_{dev} is non-zero. This implies the input/output relationship, Θ_{dev} value will switch signs four times during one rotation of the input shaft. These solutions are double-frequency periodic functions for specified deviation angles. The larger the driveline offset angle the sharper the change and the larger the amplitude of the Θ_{dev} deviation values.

Although the amplitude of the Θ_{dev} deviation is small under the influence of the α_{dev} deviation angle, the transmission plane locating device is most likely to produce greater errors about the α_{frame} axis. The transmission plane locating device is most apt to produce errors about this axis. as the maximum variation of the homokinetic plane with respect to the changes in the frame angle will occur about this axis.

The most concerning variations in the input/output relationship occur when the two deviation angles are both non-zero. The slightest combination of the η_{dev} with the α_{dev} can change the phase and increase the amplitude of the lead or lag. The mechanical tolerances in the transmission plane locating device of a CV coupling should take into account the volatility of the η_{dev} as it can have grave effects at very minute values. As the locating device is generally concerned with positioning of the transmission plane about the axis of the frame angle, perhaps additional concern should be made to accomodate the strong influence of the η_{dev} value.

Combinations of the η_{dev} and α_{dev} transmission angles prescribe all possible configurations of a general coupling with a specified transmission plane. The η_{dev} and α_{dev} transmission angles once established can be evaluated to obtain the input/output relationship. An efficient non-recursive formula for the relationship between the input and output shafts of a CV coupling, when constant-velocity constraints are not satisfied, has been presented here. A mathematical model has been derived to allow for all possible configurations of the CV joint to be evaluated.

This system offers insight on the CV Coupling's short comings and focuses on an approach to quantifying performance of specific CV coupling mechanisms. This system provides information on how precise a CV Coupling will be subject to mechanism designs and tolerances. By quantifying the input/output relationship for a CV coupling a set of standards can be established.

REFERENCES

Akivis, M. A., and V. V. Goldberg. 1972. "An Introduction to Linear Algebra & Tensors." Dover Publications, Inc., New York, ISBN 0-486-63545-7.

Bellomo, N. 1975. "Theoretical analysis of static forces and torque transmission by a class of spatial systems of rigid bodies for constant velocity transmission." *Mechanical Research Communications,* Vol.2 249-254.

Bottema, O., and B. Roth. 1979. "Theoretical Kinematics." North Holland Publishing Co., New York, 1979, ISBN 0-444-85124-0

Craig, J. J. 1986. "Introduction to Robotics." Addison-Wesley Publishing Co., Mass., ISBN 0-201-10326-5.

Duffy, J., and M. J. Gilmartin. 1979. "Displacement Analysis of Spatial 7R Mechanisms Suitable for Constant-Velocity Transmission between Parallel Shafts." *Journal of Mechanism Design ASME,* Vol.6 October 604-614.

Freudenstein, F., and E. R. Maki. 1979. "The creation of mechanisms according to kinematic structure and function." *Environment and Planning B*, Vol.6 375-391.

Hunt, K. H. 1973. "Constant-Velocity Shaft Couplings: a General Theory." Transactions, *Journal of Engineering for Industry ASME,* 95B 455-464.

Mabie, H. H. 1948. "Constant-velocity Joints with particular reference to Constant-velocity Type." *Machine Design* Vol.20, No.5 101-105.

Macielinski, J. W. 1970. "The Design and Selection of Universal Joints." *The Journal of Automotive Engineering* June, 8-14.

McCarthy, J. M. 1990. "Introduction to Theoretical Kinematics." MIT Press, Cambridge, Mass.

Miller, F. F. 1965. "Constant-Velocity Universal Ball Joints." *Machine Design* March, 184-.

Myard, F. E. 1933. "Theorie Generale: Des Joints de Transmission de Rotation." *Le Genie Civil* April, 345-.

Myard, F. E. 1933. "Les Transmissions de Rotation a Couples D'emboitment." *Le Genie Civil* June, 539-.

O'Neil, P. V. 1987. "Advanced Engineering Mathmatics 2nd edition." Wadsworth Publishing Co., California, ISBN 0-534-06792-1.

Rzeppa, A. H. 1953. "Universal Joint Drives." *Machine Design* April, 162-170.

Sandor, G. N., and A. G. Erdman. 1984. "Advanced Mechanism Design: Analysis and Synthesis Vol.2." Prentice-Hall, Inc., Englewood Cliffs, New Jersey.

Steeds, W. 1937. "Universal Joints." *The Automobile Engineer*, January, London, England, 10-12.

Sturges, E. B. 1947. "Constant-Velocity Universal Joints." *Product Engineering* July, 120-123.

Sutherland, G. H. 1976. "Finding bearing loads caused by Constant-Velocity U-Joints." *Machine Design* April, 55-59.

Taniyama, K., S. Kubo, and T. Taniguchi. 1985. "Effects of Dimensional Factors on the Life of the Rzeppa Universal Joint." *SAE Technical Paper Series #850355* Detroit, Mich., February 25-March 1, 25-32.